

Two Holes Dynamics in the Ising Antiferromagnetic Chains

S. Ehika¹ and J.O.A. Idiodi²

¹Department of physics, Ambrose Alli University, Ekpoma, Edo State, Nigeria.

²Department of Physics, University of Benin, Benin City, Nigeria.

Abstract

The t - J_z model is the strongly anisotropic limit of the t - J model which captures some general properties of the doped antiferromagnets (AF). The absence of spin fluctuations simplifies the analytical treatment of this problem and makes it possible to visualize the independent effect of hole(s) on the antiferromagnet. This paper studies the dynamics of two holes on one dimensional Ising antiferromagnetic Mott insulator. The energy of the two holes for none zero exchange J_z is calculated using exact diagonalization method. Systems with Odd number of sites N up to nine are presented. The energy of the hole is found to increase slightly in the weak coupling regime ($J_z / t \ll 1$) and sharply in the strong coupling regime ($J_z / t \gg 1$). This increase in the energy of the holes is due to the magnetic energy cost incurred in creating a ferromagnetic bond or a string of flipped spins. Comparison with the result obtained for the single hole at finite J_z shows that the energy expended by a single hole in an Ising antiferromagnet is greater than that expended by two holes in the same background. In particular, it is observed that an increase in N increases the single hole energy slightly. On the other hand, an increase in N causes a decrease in the energy of two holes for finite J_z . This means that two mobile holes in the bulk limit in one dimensional antiferromagnet can minimize their energy and so maintain a smooth coherent motion. The implication of this result for superconductivity of doped Mott insulators is discussed.

Keywords: Ising antiferromagnet, confinement, bulk limit, exact diagonalization and hole pairing.

1.0 Introduction

Interest in nonphonon-induced pairing has been stimulated by the discovery of the copper-oxide-based or cuprate superconductors [1]. Possible mechanisms for superconductivity in the cuprates are still the subject of considerable debate and further research. Certain aspects common to all materials have been identified [2]. Similarities between the antiferromagnetic low-temperature state of the undoped materials and the superconducting state that emerges upon doping, primarily the $d_{x^2-y^2}$ orbital state of the Cu^{2+} ions, suggest that electron-electron interactions are more significant than electron-phonon interactions in cuprates – making the superconductivity unconventional.

Due to strong onsite Coulomb repulsion, at half filling electronic motions are frozen, leaving spins dynamics as the only degree of freedom. The magnetic properties of these half-filled (undoped) systems are well described by the isotropic spin-1/2 Heisenberg model [3]. The localization of these electrons even in the absence of disorder gives rise to a gapped electronic state known as the Mott insulator [4]. The fact that these unconventional insulators produce superconductivity when holes or vacancies of optimum concentration are introduced into them implies that holes are not static in the antiferromagnetic background, but mobile. The motion of these holes can produce a local distortion of the spin background by altering the spin configurations [3].

Besides the two dimensional Mott insulators which become superconducting on doping, there have also been rigorous and intense researches on one and quasi-one dimensional systems. The motivation for researches on one and quasi-one

Corresponding author: S. Ehika, E-mail: ehikasimon@yahoo.com, Tel.: +2348074478911

dimensional systems is because of the intriguing phenomena that have been discovered theoretically and experimentally in them. For instance, the injection of a single hole into quasi-one dimensional Mott insulators such as Sr_2CuO_3 and SrCuO_2 has given rise to Spin-charge separations [5-8]. Furthermore, the close structural and electronic relationship of these materials to the high-temperature superconductors (HTSC), and the known instabilities of the HTSC towards one-dimensional phenomena, forms a background which provides a strong motivation for close scrutiny [9-12]. Low dimensional systems such as ladder systems have also been used as a fantastic playground to observe the effect of hole dynamics on antiferromagnetically ordered spin background. For instance, self-localization that invalidates the quasi-particle picture has been observed in antiferromagnetic ladder systems [13]. This self-localization of a single hole which arises from quantum destructive interference of the phase string signs hidden in the t - J ladders can be removed by pairing two holes [14]. The hole pairing mechanism is supported by both theoretical and experimental reports [15-17]. However, the argument put forward by some theoretical Physicist did not seem to favour hole pairing [18, 19]. Trugman [18] also argued that a single hole in an antiferromagnet can avoid being trapped if it follows a complicated path that translates it into a degenerate vacuum. But recent discovery of string excitations in refs.[20-22] from ARPES studies of cuprates seems to be in support of the string picture proposed in ref.[15] in the intermediate coupling regime. It is therefore obvious that there is lack of consensus regarding the dynamics of both single and two holes in an antiferromagnet. This field is still evolving with theoretical and experimental researches geared towards addressing some of the problems of this hole(s) dynamics.

The aim of the present work is to study the propagation of two holes in 1D t - J_z model with exact diagonalization method. It is hoped that this simplified model will shed more light on some elusive aspect of two holes dynamics and provide further evidence in support of hole pairing as a mechanism for superconductivity. The rest of the paper is organized as follows: In section 2, the Ising model in 1D is presented and an effective Hamiltonian describing two holes dynamics in the midst of the Ising interaction term is introduced. In section 3, we derive a formula for the size of the Hilbert space of two holes in the Ising antiferromagnet. In section 4, the dynamics of two holes in finite antiferromagnetic chains are studied with exact diagonalization method. The result of the numerical ground state energy of two holes as a function of the coupling constant J_z is presented in section 5. A brief conclusion will close the paper in section 6.

2.0 The Ising Antiferromagnetic Model

The Hamiltonian describing hole dynamics in an Ising model is a simple generalization of the t - J model where only the S^z component of the spins are retained. In 1D this model reads

$$H = -t \sum_{i\sigma} [C_{i\sigma}^\dagger C_{i+1\sigma} + C_{i+1\sigma}^\dagger C_{i\sigma}] + J_z \sum_i S_i^z S_{i+1}^z. \quad (1)$$

Here, $C_{i\sigma}^\dagger$ ($C_{i\sigma}$) is the creation (annihilation) operator of an electron with spin σ at the lattice site i ; $S_i^z = 1/2(c_{i\uparrow}^\dagger c_{i\uparrow} - c_{i\downarrow}^\dagger c_{i\downarrow})$ is the Ising component of the antiferromagnetic spin interaction; t is the effective transfer integral (or the kinetic energy term) and J_z is the antiferromagnetic exchange energy for a pair of nearest neighbour spins. In this model, the constraint of no double occupancy of any site is understood.

In this work, odd chains with periodic boundary conditions are considered. In the absence of a hole, the ground state of the $t - J_z$ model is a perfect Néel state with energy given by

$$E_N = -\frac{J_z(N-2)}{4} \quad (2)$$

where N is the number of sites and $N-2$ is the net number of antiferromagnetic bonds. The two antiferromagnetic states (Néel state) of the undoped chain are $|1\uparrow, 2\downarrow, \dots, N\uparrow\rangle$ and $|1\downarrow, 2\uparrow, \dots, N\downarrow\rangle$. Hence, the Néel state is already in the subspace of $S_{tot}^z = 1/2$ or the subspace of $S_{tot}^z = -1/2$. Out of these two states obtained by translation of one lattice vector, two arbitrary spins are selected. The annihilation of these two arbitrary electrons in the Néel state defines the starting state, i.e. $|0\rangle = c_{i\sigma} c_{j\sigma'} |N\rangle$ (where σ' may be the same or different from σ). When the Hamiltonian in (1) acts on $|0\rangle$, states which can uniquely be labelled by the position of the hole $|R\rangle$ are generated.

In order to create two holes, two electrons must be annihilated. The annihilation of the two electrons in the Néel state of subspace $S_{tot}^z = 1/2$ will generate three possible subspaces. These include the subspace of $S_{tot}^z = 1/2$ arising from the arbitrary annihilation of two anti-aligned spins; the subspace $S_{tot}^z = -1/2$ arising from the annihilation of the two ferromagnetically aligned up spins; and the subspace $S_{tot}^z = 3/2$ arising from the annihilation of the two ferromagnetically

aligned down spins. Also, the annihilation of the two electrons in the Néel state of subspace $S_{tot}^z = -1/2$ will generate three possible subspaces. These include the subspace $S_{tot}^z = -1/2$ arising from the arbitrary annihilation of the two anti-aligned spins; the subspace $S_{tot}^z = 1/2$ arising from the annihilation of the two ferromagnetically aligned down spins; and the subspace $S_{tot}^z = -3/2$ arising from the annihilation of the two ferromagnetically aligned up spins. In this work we shall investigate the dynamics of two holes in the Néel state of subspace $S_{tot}^z = 1/2$.

The following Hamiltonian for the dynamics of two holes in finite one dimensional antiferromagnet is proposed.

$$H'|\vec{R}\rangle = -t[|\vec{R}_1\rangle + |\vec{R}_2\rangle] + \epsilon'|\vec{R}\rangle \tag{3}$$

where H' , ϵ' and \vec{R} are respectively given by

$$\epsilon' = \epsilon_t - \epsilon_N \tag{4}$$

$$H' = H - H_{I\text{sing}} \tag{5}$$

$$\vec{R} = \vec{R}_2 - \vec{R}_1 \tag{6}$$

Here ϵ_N is the energy of the Néel state; ϵ_t is the energy of the system with holes; \vec{R}_1 and \vec{R}_2 are the position vectors of the two holes and $H_{I\text{sing}}$ is the Hamiltonian for the Néel state, describing spin interactions in the absence of quantum spin fluctuation. By considering the dynamics of the ferromagnetic bond produced as a result of the motion of the two holes as well as the relative positions of the holes, the following operations are possible

$$H'|R\rangle = -t[|R_1 - 1\rangle + |R_2 + 1\rangle] + \frac{J_z}{4}|R\rangle \tag{7}$$

$$H'|R\rangle = -t[|R_1 - 1\rangle + |R_1 + 1\rangle + |R_2 - 1\rangle + |R_2 + 1\rangle] + \frac{J_z}{2}|R\rangle \tag{8}$$

$$H'|R\rangle = -t[|R_1 - 1\rangle + |R_1 + 1\rangle + |R_2 - 1\rangle + |R_2 + 1\rangle] + J_z|R\rangle \tag{9}$$

$$H'|R\rangle = -t[|R_1 - 1\rangle + |R_2 + 1\rangle] + \frac{3J_z}{4}|R\rangle \tag{10}$$

The operation in (7) is obtained when the two holes are at their “birth sites” (i.e. when either of the holes has not hopped). Here, the first hole is placed at $R_1 = 0$ (i.e. at the origin), while the second hole is placed at R_2 , a distance of one lattice spacing from R_1 (i.e. both holes are nearest neighbour). In this way, the number of degrees of freedom for the two holes is reduced to two (that for a single hole). The operation in (8) is obtained when the holes propagate in such a way that leaves a given chain completely devoid of paired holes and a ferromagnetic bond. The operation in (9) arises from chains with ferromagnetic bond, but devoid of paired holes. The operation in (10) arises from chains with both paired holes and a ferromagnetic bond.

The translational invariance property of the $t - J_z$ model can be utilized in reducing the size of the Hilbert space for two holes. This means that any two-hole state with definite momentum k and spin σ' or σ can be written as:

$$|\psi_k\rangle = \frac{1}{\sqrt{N}} \sum_{r=0}^{N-1} e^{-ikr} T_N^r c_{0\uparrow} |\sigma_0\rangle, \tag{11}$$

where $|\sigma_0\rangle$ is a suitable spin state with the spins at the origin $r = 0$ fixed to \uparrow and T_N is the spin translation operator defined by the transformation property

$$T_N S_R T_N^{-1} = S_{R+1} \tag{12}$$

where periodic boundary conditions (PBC) over the N sites are assumed in order to define the effect of translation at the rightmost site.

3.0 Hilbert Space for Two Holes In Ising Antiferromagnet

In this section, the size of the Hilbert space for two holes propagating in the Néel state of $S_{tot}^z = 1/2$ will be obtained. Fig. 1 represents N -site chains with two holes occupying the first and second sites.

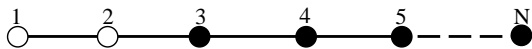


Fig.1. Arrangement of two holes and electrons on N-site chains. The shaded circles represent electrons, while the empty circles represent electrons.

The arbitrary chosen birth state of the two holes denoted by $|0\rangle$ is given by

$$|0\rangle = c_{1\uparrow}c_{2\downarrow}|N\rangle = c_{1\uparrow}c_{2\downarrow}|1\uparrow, 2\downarrow, 3\uparrow, 4\downarrow, 5\uparrow \dots N\uparrow\rangle = |1, 2, 3\uparrow, 4\downarrow, 5\uparrow \dots N\uparrow\rangle \quad (13)$$

The positions of the two holes are chosen in such a way that they are at nearest neighbour (NN) sites. This choice of birth state for the holes though convenient, is arbitrary and not based on strict or rigid rules. If any of the two holes are allowed to move with the constraint that the N^{th} lattice site is not occupied and the constraint of no double occupancy of any site is adhered to, its degrees of freedom will be $N-3$. The former constraint imposed on the dynamics of the two holes ensures that the holes' states are not double counted. The 1st, 2nd and $(N-3)^{\text{th}}$ hops of the hole at site 2 are respectively given by (14), (15) and (16).

$$|1\rangle = |1, 2\uparrow, 3, 4\downarrow, 5\uparrow \dots N\uparrow\rangle \quad (14)$$

$$|2\rangle = |1, 2\uparrow, 3\downarrow, 4, 5\uparrow \dots N\uparrow\rangle \quad (15)$$

$$|N-3\rangle = |1, 2\uparrow, 3\downarrow, 4\uparrow, 5\uparrow \dots (N-1), N\uparrow\rangle \quad (16)$$

Propagating in the same direction as the first hole originally at site 2, the second hole at site 1 must make 1, 2 and $(N-3)$ hops in order to pair with the first hole. This means that the total states generated by the second hole can be obtained from the arithmetic series

$$S_N = \frac{N}{2}[2a + (N-1)d] \quad (17)$$

Here, N is the number of sites; the first term in the series is 1; d the common difference is also 1. But the last term of an arithmetic progression is given by

$$l = a + (N-1)d \quad (18)$$

Hence, (17) becomes

$$S_N = \frac{N}{2}(a+l) \quad (19)$$

The last term l is given by

$$l = N-3 \quad (20)$$

Hence (19) becomes

$$S_N = \frac{N}{2}(1+N-3) \quad (20)$$

But the sum of all the states from $|0\rangle$ to $|N-3\rangle$ equals $N-3+1 = N-2$. Adding this to (20) gives

$$S_N = \frac{N}{2}(1+N-3) + N-2 = \frac{1}{2}(N-1)(N-2) = \frac{N!}{2N(N-3)!} \quad (21)$$

The states $|0\rangle, |1\rangle, |2\rangle$, etc are representative of groups of normalized state vectors obtained by making use of the translational invariance of the t - J_z model. Thus, (21) gives the number of normalized state vectors obtained by making use of the translational symmetry discussed in section 2. Since translational symmetries give $1/N$ reduction in the size of the system, the size of the Hilbert space for two mobile holes in Ising antiferromagnet gives

$$S_N = \frac{N!}{2(N-3)!} \quad (22)$$

4.0 The Dynamics of Two Holes In a Finite Antiferromagnetic Chain

This section presents the dynamics of two holes in one dimensional antiferromagnetic chain.

4.1 Five -Site Chain

A five-site chain with three electrons and two holes condition is illustrated in Fig. 2.

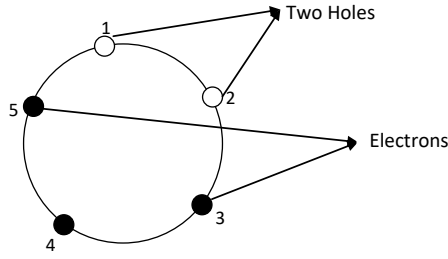


Fig. 2: A five- site chain with two holes and three electrons subjected to periodic boundary conditions.

The two antiferromagnetic states (Neel state) of the undoped chain are $|1 \uparrow, 2 \downarrow, 3 \uparrow, 4 \downarrow, 5 \uparrow\rangle$ and $|1 \downarrow, 2 \uparrow, 3 \downarrow, 4 \uparrow, 5 \downarrow\rangle$. The

birth state denoted by $|0\rangle$ is given by

$$|0\rangle = c_{1\uparrow}c_{2\downarrow}|N\rangle = c_{1\uparrow}c_{2\downarrow}|1 \uparrow, 2 \downarrow, 3 \uparrow, 4 \downarrow, 5 \uparrow\rangle = |1, 2, 3 \uparrow, 4 \downarrow, 5 \uparrow\rangle \quad (23)$$

From (22), the size of the Hilbert space of this system is $S_5 = \frac{5!}{2(5-3)!} = \frac{5!}{4} = 30$. This can easily be reduced to 6 normalized

states by using (11). The other electronic states which are shown below can be obtained from $|0\rangle$ by hopping and translating the holes one lattice spacing.

$$|\phi_0\rangle = \frac{1}{\sqrt{5}} \left[|1, 2, 3 \uparrow, 4 \downarrow, 5 \uparrow\rangle + |1 \uparrow, 2, 3, 4 \uparrow, 5 \downarrow\rangle + |1 \downarrow, 2 \uparrow, 3, 4, 5 \uparrow\rangle \right. \\ \left. + |1 \uparrow, 2 \downarrow, 3 \uparrow, 4, 5\rangle + |1, 2 \uparrow, 3 \downarrow, 4 \uparrow, 5\rangle \right]$$

$$|\phi_1\rangle = \frac{1}{\sqrt{5}} \left[|1, 2 \uparrow, 3, 4 \downarrow, 5 \uparrow\rangle + |1 \uparrow, 2, 3 \uparrow, 4, 5 \downarrow\rangle + |1 \downarrow, 2 \uparrow, 3, 4 \uparrow, 5\rangle \right. \\ \left. + |1, 2 \downarrow, 3 \uparrow, 4, 5 \uparrow\rangle + |1 \uparrow, 2, 3 \downarrow, 4 \uparrow, 5\rangle \right]$$

$$|\phi_2\rangle = \frac{1}{\sqrt{5}} \left[|1, 2 \uparrow, 3 \downarrow, 4, 5 \uparrow\rangle + |1 \uparrow, 2, 3 \uparrow, 4 \downarrow, 5\rangle + |1, 2 \uparrow, 3, 4 \uparrow, 5 \downarrow\rangle \right. \\ \left. + |1 \downarrow, 2, 3 \uparrow, 4, 5 \uparrow\rangle + |1 \uparrow, 2 \downarrow, 3, 4 \uparrow, 5\rangle \right]$$

$$|\phi_3\rangle = \frac{1}{\sqrt{5}} \left[|1 \uparrow, 2, 3, 4 \downarrow, 5 \uparrow\rangle + |1 \uparrow, 2 \uparrow, 3, 4, 5 \downarrow\rangle + |1 \downarrow, 2 \uparrow, 3 \uparrow, 4, 5\rangle \right. \\ \left. + |1, 2 \downarrow, 3 \uparrow, 4 \uparrow, 5\rangle + |1, 2, 3 \downarrow, 4 \uparrow, 5 \uparrow\rangle \right]$$

$$|\phi_4\rangle = \frac{1}{\sqrt{5}} \left[|1 \uparrow, 2, 3 \downarrow, 4, 5 \uparrow\rangle + |1 \uparrow, 2 \uparrow, 3, 4 \downarrow, 5\rangle + |1, 2 \uparrow, 3 \uparrow, 4, 5 \downarrow\rangle \right. \\ \left. + |1 \downarrow, 2, 3 \uparrow, 4 \uparrow, 5\rangle + |1, 2 \downarrow, 3, 4 \uparrow, 5 \uparrow\rangle \right]$$

$$|\phi_5\rangle = \frac{1}{\sqrt{5}} \left[|1 \uparrow, 2 \downarrow, 3, 4, 5 \uparrow\rangle + |1 \uparrow, 2 \uparrow, 3 \downarrow, 4, 5\rangle + |1, 2 \uparrow, 3 \uparrow, 4 \downarrow, 5\rangle \right. \\ \left. + |1, 2, 3 \uparrow, 4 \uparrow, 5 \downarrow\rangle + |1 \downarrow, 2, 3, 4 \uparrow, 5 \uparrow\rangle \right]$$

The action of H' on the reduced Hilbert space, gives

$$H'|\phi_0\rangle = -t|\phi_1\rangle - t|\phi_2\rangle + \frac{J_z}{4}|\phi_0\rangle$$

$$H'|\phi_1\rangle = -t|\phi_0\rangle - t|\phi_2\rangle - t|\phi_3\rangle - t|\phi_4\rangle + \frac{J_z}{2}|\phi_1\rangle$$

$$H'|\phi_2\rangle = -t|\phi_0\rangle - t|\phi_1\rangle - t|\phi_4\rangle - t|\phi_5\rangle + \frac{J_z}{2}|\phi_2\rangle$$

$$H'|\phi_3\rangle = -t|\phi_1\rangle - t|\phi_4\rangle + \frac{3J_z}{4}|\phi_3\rangle$$

$$H'|\phi_4\rangle = -t|\phi_1\rangle - t|\phi_2\rangle - t|\phi_3\rangle - t|\phi_4\rangle + J_z|\phi_4\rangle$$

$$H'|\phi_5\rangle = -t|\phi_2\rangle - t|\phi_4\rangle + \frac{3J_z}{4}|\phi_5\rangle$$

The Hamiltonian matrix for this operation is given by

$$H' = \begin{bmatrix} \frac{J_z}{4} & -t & -t & 0 & 0 & 0 \\ -t & \frac{J_z}{2} & -t & -t & -t & 0 \\ -t & -t & \frac{J_z}{2} & 0 & -t & -t \\ 0 & -t & 0 & \frac{3J_z}{4} & -t & 0 \\ 0 & -t & -t & -t & J_z & -t \\ 0 & 0 & -t & 0 & -t & \frac{3J_z}{4} \end{bmatrix} \quad (24)$$

4.2 Seven -Site Chain

A seven-site chain with five electrons and two holes is illustrated in Fig. 3.

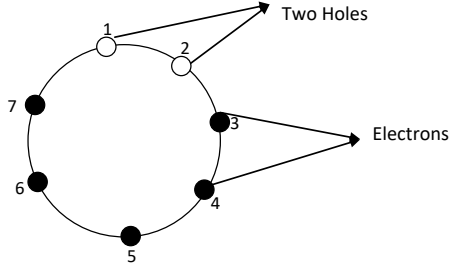


Fig 3: A Seven-site chain with two holes and five electrons subjected to periodic boundary conditions.

The two antiferromagnetic states (Neél state) of the undoped chain are $|1 \uparrow, 2 \downarrow, 3 \uparrow, 4 \downarrow, 5 \uparrow, 6 \downarrow, 7 \uparrow\rangle$ and $|1 \downarrow, 2 \uparrow, 3 \downarrow, 4 \uparrow, 5 \downarrow, 6 \uparrow, 7 \downarrow\rangle$

The annihilation of these two anti-aligned spins at site 1 and 2 defines the starting state or the birth state of the holes. This birth state is given by

$$|0\rangle = c_{1\uparrow}c_{2\downarrow}|N\rangle = c_{1\uparrow}c_{2\downarrow}|1 \uparrow, 2 \downarrow, 3 \uparrow, 4 \downarrow, 5 \uparrow, 6 \downarrow, 7 \uparrow\rangle = |1, 2, 3 \uparrow, 4 \downarrow, 5 \uparrow, 6 \downarrow, 7 \uparrow\rangle \quad (25)$$

From (22), the size of the Hilbert space of this system is $S_7 = \frac{7!}{2(7-3)!} = \frac{7!}{2 \times 4!} = 105$. This can easily be reduced to 15

normalized states by using (11). These 15 normalized states obtained from $|0\rangle$ are shown below.

$$|\phi_0\rangle = \frac{1}{\sqrt{7}} \left[\begin{array}{l} |1, 2, 3 \uparrow, 4 \downarrow, 5 \uparrow, 6 \downarrow, 7 \uparrow\rangle + |1 \uparrow, 2, 3, 4 \uparrow, 5 \downarrow, 6 \uparrow, 7 \downarrow\rangle + |1 \downarrow, 2 \uparrow, 3, 4, 5 \uparrow, 6 \downarrow, 7 \uparrow\rangle \\ + |1 \uparrow, 2 \downarrow, 3 \uparrow, 4, 5, 6 \uparrow, 7 \downarrow\rangle + |1 \downarrow, 2 \uparrow, 3 \downarrow, 4 \uparrow, 5, 6, 7 \uparrow\rangle + |1 \uparrow, 2 \downarrow, 3 \uparrow, 4 \downarrow, 5 \uparrow, 6, 7\rangle \\ + |1, 2 \uparrow, 3 \downarrow, 4 \uparrow, 5 \downarrow, 6 \uparrow, 7\rangle \end{array} \right]$$

$$|\phi_1\rangle = \frac{1}{\sqrt{7}} \left[\begin{array}{l} |1, 2 \uparrow, 3, 4 \downarrow, 5 \uparrow, 6 \downarrow, 7 \uparrow\rangle + |1 \uparrow, 2, 3 \uparrow, 4, 5 \downarrow, 6 \uparrow, 7 \downarrow\rangle + |1 \downarrow, 2 \uparrow, 3, 4 \uparrow, 5, 6 \downarrow, 7 \uparrow\rangle \\ + |1 \uparrow, 2 \downarrow, 3 \uparrow, 4, 5 \uparrow, 6, 7 \downarrow\rangle + |1 \downarrow, 2 \uparrow, 3 \downarrow, 4 \uparrow, 5, 6 \uparrow, 7\rangle + |1, 2 \downarrow, 3 \uparrow, 4 \downarrow, 5 \uparrow, 6, 7 \uparrow\rangle \\ + |1 \uparrow, 2, 3 \downarrow, 4 \uparrow, 5 \downarrow, 6 \uparrow, 7\rangle \end{array} \right]$$

$$|\phi_2\rangle = \frac{1}{\sqrt{7}} \left[\begin{array}{l} |1, 2 \uparrow, 3 \downarrow, 4, 5 \uparrow, 6 \downarrow, 7 \uparrow\rangle + |1 \uparrow, 2, 3 \uparrow, 4 \downarrow, 5, 6 \uparrow, 7 \downarrow\rangle + |1 \downarrow, 2 \uparrow, 3, 4 \uparrow, 5 \downarrow, 6, 7 \uparrow\rangle \\ + |1 \uparrow, 2 \downarrow, 3 \uparrow, 4, 5 \uparrow, 6 \downarrow, 7\rangle + |1, 2 \uparrow, 3 \downarrow, 4 \uparrow, 5, 6 \uparrow, 7 \downarrow\rangle + |1 \downarrow, 2, 3 \uparrow, 4 \downarrow, 5 \uparrow, 6, 7 \uparrow\rangle \\ + |1 \uparrow, 2 \downarrow, 3, 4 \uparrow, 5 \downarrow, 6 \uparrow, 7\rangle \end{array} \right]$$

$$|\phi_3\rangle = \frac{1}{\sqrt{7}} \left[\begin{array}{l} |1, 2 \uparrow, 3 \downarrow, 4 \uparrow, 5, 6 \downarrow, 7 \uparrow\rangle + |1 \uparrow, 2, 3 \uparrow, 4 \downarrow, 5 \uparrow, 6, 7 \downarrow\rangle + |1 \downarrow, 2 \uparrow, 3, 4 \uparrow, 5 \downarrow, 6 \uparrow, 7\rangle \\ + |1, 2 \downarrow, 3 \uparrow, 4, 5 \uparrow, 6 \downarrow, 7 \uparrow\rangle + |1 \uparrow, 2, 3 \downarrow, 4 \uparrow, 5, 6 \uparrow, 7 \downarrow\rangle + |1 \downarrow, 2 \uparrow, 3, 4 \downarrow, 5 \uparrow, 6, 7 \uparrow\rangle \\ + |1 \uparrow, 2 \downarrow, 3 \uparrow, 4, 5 \downarrow, 6 \uparrow, 7\rangle \end{array} \right]$$

$$\begin{aligned}
 H'|\phi_0\rangle &= -t|\phi_1\rangle - t|\phi_4\rangle + \frac{J_z}{4}|\phi_0\rangle \\
 H'|\phi_1\rangle &= -t|\phi_0\rangle - t|\phi_2\rangle - t|\phi_5\rangle - t|\phi_{11}\rangle + \frac{J_z}{2}|\phi_1\rangle \\
 H'|\phi_2\rangle &= -t|\phi_1\rangle - t|\phi_3\rangle - t|\phi_6\rangle - t|\phi_{12}\rangle + \frac{J_z}{2}|\phi_2\rangle \\
 H'|\phi_3\rangle &= -t|\phi_2\rangle - t|\phi_4\rangle - t|\phi_8\rangle - t|\phi_{13}\rangle + \frac{J_z}{2}|\phi_3\rangle \\
 H'|\phi_4\rangle &= -t|\phi_0\rangle - t|\phi_3\rangle - t|\phi_{11}\rangle - t|\phi_{14}\rangle + \frac{J_z}{2}|\phi_4\rangle \\
 H'|\phi_5\rangle &= -t|\phi_1\rangle - t|\phi_6\rangle + \frac{3J_z}{4}|\phi_4\rangle \\
 H'|\phi_6\rangle &= -t|\phi_2\rangle - t|\phi_5\rangle - t|\phi_7\rangle - t|\phi_8\rangle + J_z|\phi_6\rangle \\
 H'|\phi_7\rangle &= -t|\phi_6\rangle - t|\phi_9\rangle + \frac{3J_z}{4}|\phi_7\rangle \\
 H'|\phi_8\rangle &= -t|\phi_3\rangle - t|\phi_6\rangle - t|\phi_9\rangle - t|\phi_{11}\rangle + J_z|\phi_8\rangle \\
 H'|\phi_9\rangle &= -t|\phi_7\rangle - t|\phi_8\rangle - t|\phi_{10}\rangle - t|\phi_{12}\rangle + J_z|\phi_9\rangle \\
 H'|\phi_{10}\rangle &= -t|\phi_9\rangle - t|\phi_{13}\rangle + \frac{3J_z}{4}|\phi_{10}\rangle \\
 H'|\phi_{11}\rangle &= -t|\phi_1\rangle - t|\phi_4\rangle - t|\phi_8\rangle - t|\phi_{12}\rangle + J_z|\phi_{11}\rangle \\
 H'|\phi_{12}\rangle &= -t|\phi_2\rangle - t|\phi_9\rangle - t|\phi_{11}\rangle - t|\phi_{13}\rangle + J_z|\phi_{13}\rangle \\
 H'|\phi_{13}\rangle &= -t|\phi_3\rangle - t|\phi_{10}\rangle - t|\phi_{12}\rangle - t|\phi_{13}\rangle + J_z|\phi_{13}\rangle \\
 H'|\phi_{14}\rangle &= -t|\phi_4\rangle - t|\phi_{13}\rangle + \frac{3J_z}{4}|\phi_{14}\rangle
 \end{aligned}$$

The Hamiltonian matrix for this operation is given by

$$H' = \begin{pmatrix}
 \frac{J_z}{4} & -t & 0 & 0 & -t & 0 & 0 & 0 & 0 & 0 & 0 & 0 & 0 & 0 & 0 \\
 -t & \frac{J_z}{2} & -t & 0 & 0 & -t & 0 & 0 & 0 & 0 & 0 & -t & 0 & 0 & 0 \\
 0 & -t & \frac{J_z}{2} & -t & 0 & 0 & -t & 0 & 0 & 0 & 0 & 0 & -t & 0 & 0 \\
 0 & 0 & -t & \frac{J_z}{2} & -t & 0 & 0 & 0 & -t & 0 & 0 & 0 & 0 & -t & 0 \\
 -t & 0 & 0 & -t & \frac{J_z}{2} & 0 & 0 & 0 & 0 & 0 & 0 & -t & 0 & 0 & -t \\
 0 & -t & 0 & 0 & 0 & \frac{3J_z}{4} & -t & 0 & 0 & 0 & 0 & 0 & 0 & 0 & 0 \\
 0 & 0 & -t & 0 & 0 & -t & J_z & -t & -t & 0 & 0 & 0 & 0 & 0 & 0 \\
 0 & 0 & 0 & 0 & 0 & 0 & -t & \frac{3J_z}{4} & 0 & -t & 0 & 0 & 0 & 0 & 0 \\
 0 & 0 & 0 & -t & 0 & 0 & -t & 0 & J_z & -t & 0 & -t & 0 & 0 & 0 \\
 0 & 0 & 0 & 0 & 0 & 0 & 0 & -t & -t & J_z & -t & 0 & -t & 0 & 0 \\
 0 & 0 & 0 & 0 & 0 & 0 & 0 & 0 & 0 & -t & \frac{3J_z}{4} & 0 & 0 & -t & 0 \\
 0 & -t & 0 & 0 & -t & 0 & 0 & 0 & -t & 0 & 0 & J_z & -t & 0 & 0 \\
 0 & 0 & -t & 0 & 0 & 0 & 0 & 0 & 0 & -t & 0 & -t & J_z & -t & 0 \\
 0 & 0 & 0 & -t & 0 & 0 & 0 & 0 & 0 & 0 & -t & 0 & -t & J_z & -t \\
 0 & 0 & 0 & 0 & -t & 0 & 0 & 0 & 0 & 0 & 0 & 0 & 0 & -t & \frac{3J_z}{4}
 \end{pmatrix} \tag{26}$$

4.3 Nine-Site Chain

A nine-site chain with seven electrons and two holes s is illustrated in Fig. 4.

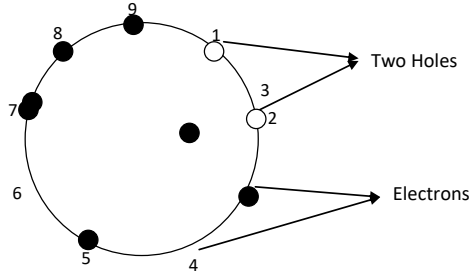


Fig. 4: A nine- site chain consisting of two holes and seven electrons with periodic boundary conditions.

The two antiferromagnetic states (Neél state) of the undoped chain are $|1 \uparrow, 2 \downarrow, 3 \uparrow, 4 \downarrow, 5 \uparrow, 6 \downarrow, 7 \uparrow, 8 \downarrow, 9 \uparrow\rangle$ and $|1 \downarrow, 2 \uparrow, 3 \downarrow, 4 \uparrow, 5 \downarrow, 6 \uparrow, 7 \downarrow, 8 \uparrow, 9 \downarrow\rangle$. The birth state is given by

$$|0\rangle = c_{1\uparrow}c_{2\downarrow}|N\rangle = c_{1\downarrow}c_{2\uparrow}|1 \uparrow, 2 \downarrow, 3 \uparrow, 4 \downarrow, 5 \uparrow, 6 \downarrow, 7 \uparrow, 8 \downarrow, 9 \uparrow\rangle = |1, 2, 3 \uparrow, 4 \downarrow, 5 \uparrow, 6 \downarrow, 7 \uparrow, 8 \downarrow, 9 \uparrow\rangle \quad (27)$$

The size of the Hilbert space of this system is $S_9 = \frac{9!}{2(9-3)!} = \frac{9!}{2 \times 6!} = 252$. This can easily be reduced to 28 normalized states

according to (21) by using (11). These 28 normalized states obtained from $|0\rangle$ are shown below.

$$\begin{aligned}
 |\phi_0\rangle &= \frac{1}{\sqrt{9}} \left[\begin{aligned} &|1, 2, 3 \uparrow, 4 \downarrow, 5 \uparrow, 6 \downarrow, 7 \uparrow, 8 \downarrow, 9 \uparrow\rangle + |1 \uparrow, 2, 3, 4 \uparrow, 5 \downarrow, 6 \uparrow, 7 \downarrow, 8 \uparrow, 9 \downarrow\rangle \\ &+ |1 \downarrow, 2 \uparrow, 3, 4, 5 \uparrow, 6 \downarrow, 7 \uparrow, 8 \downarrow, 9 \uparrow\rangle + |1 \uparrow, 2 \downarrow, 3 \uparrow, 4, 5, 6 \uparrow, 7 \downarrow, 8 \uparrow, 9 \downarrow\rangle \\ &+ |1 \downarrow, 2 \uparrow, 3 \downarrow, 4 \uparrow, 5, 6, 7 \uparrow, 8 \downarrow, 9 \uparrow\rangle + |1 \uparrow, 2 \downarrow, 3 \uparrow, 4 \downarrow, 5 \uparrow, 6, 7, 8 \uparrow, 9 \downarrow\rangle \\ &+ |1 \downarrow, 2 \uparrow, 3 \downarrow, 4 \uparrow, 5 \downarrow, 6 \uparrow, 7, 8, 9 \uparrow\rangle + |1 \uparrow, 2 \downarrow, 3 \uparrow, 4 \downarrow, 5 \uparrow, 6 \downarrow, 7 \uparrow, 8, 9\rangle \\ &+ |1, 2 \uparrow, 3 \downarrow, 4 \uparrow, 5 \downarrow, 6 \uparrow, 7 \downarrow, 8 \uparrow, 9\rangle \end{aligned} \right] \\
 |\phi_1\rangle &= \frac{1}{\sqrt{9}} \left[\begin{aligned} &|1, 2 \uparrow, 3, 4 \downarrow, 5 \uparrow, 6 \downarrow, 7 \uparrow, 8 \downarrow, 9 \uparrow\rangle + |1 \uparrow, 2, 3 \uparrow, 4, 5 \downarrow, 6 \uparrow, 7 \downarrow, 8 \uparrow, 9 \downarrow\rangle \\ &+ |1 \downarrow, 2 \uparrow, 3, 4 \uparrow, 5, 6 \downarrow, 7 \uparrow, 8 \downarrow, 9 \uparrow\rangle + |1 \uparrow, 2 \downarrow, 3 \uparrow, 4, 5 \uparrow, 6, 7 \downarrow, 8 \uparrow, 9 \downarrow\rangle \\ &+ |1 \downarrow, 2 \uparrow, 3 \downarrow, 4 \uparrow, 5, 6 \uparrow, 7, 8 \downarrow, 9 \uparrow\rangle + |1 \uparrow, 2 \downarrow, 3 \uparrow, 4 \downarrow, 5 \uparrow, 6, 7 \uparrow, 8, 9 \downarrow\rangle \\ &+ |1 \uparrow, 2, 3 \downarrow, 4 \uparrow, 5 \downarrow, 6 \uparrow, 7 \downarrow, 8 \uparrow, 9\rangle \end{aligned} \right] \\
 |\phi_2\rangle &= \frac{1}{\sqrt{9}} \left[\begin{aligned} &|1, 2 \uparrow, 3 \downarrow, 4, 5 \uparrow, 6 \downarrow, 7 \uparrow, 8 \downarrow, 9 \uparrow\rangle + |1 \uparrow, 2, 3 \uparrow, 4 \downarrow, 5, 6 \uparrow, 7 \downarrow, 8 \uparrow, 9 \downarrow\rangle \\ &+ |1 \downarrow, 2 \uparrow, 3, 4 \uparrow, 5 \downarrow, 6, 7 \uparrow, 8 \downarrow, 9 \uparrow\rangle + |1 \uparrow, 2 \downarrow, 3 \uparrow, 4, 5 \uparrow, 6 \downarrow, 7, 8 \uparrow, 9 \downarrow\rangle \\ &+ |1 \downarrow, 2 \uparrow, 3 \downarrow, 4 \uparrow, 5, 6 \uparrow, 7 \downarrow, 8, 9 \uparrow\rangle + |1 \uparrow, 2 \downarrow, 3 \uparrow, 4 \downarrow, 5 \uparrow, 6, 7 \uparrow, 8 \downarrow, 9\rangle \\ &+ |1 \uparrow, 2 \downarrow, 3, 4 \uparrow, 5 \downarrow, 6 \uparrow, 7 \downarrow, 8 \uparrow, 9\rangle \end{aligned} \right] \\
 |\phi_3\rangle &= \frac{1}{\sqrt{9}} \left[\begin{aligned} &|1, 2 \uparrow, 3 \downarrow, 4 \uparrow, 5, 6 \downarrow, 7 \uparrow, 8 \downarrow, 9 \uparrow\rangle + |1 \uparrow, 2, 3 \uparrow, 4 \downarrow, 5 \uparrow, 6, 7 \downarrow, 8 \uparrow, 9 \downarrow\rangle \\ &+ |1 \downarrow, 2 \uparrow, 3, 4 \uparrow, 5 \downarrow, 6 \uparrow, 7, 8 \downarrow, 9 \uparrow\rangle + |1 \uparrow, 2 \downarrow, 3 \uparrow, 4, 5 \uparrow, 6 \downarrow, 7 \uparrow, 8, 9 \downarrow\rangle \\ &+ |1 \downarrow, 2 \uparrow, 3 \downarrow, 4 \uparrow, 5, 6 \uparrow, 7 \downarrow, 8 \uparrow, 9\rangle + |1, 2 \downarrow, 3 \uparrow, 4 \downarrow, 5 \uparrow, 6, 7 \uparrow, 8 \downarrow, 9 \uparrow\rangle \\ &+ |1 \uparrow, 2, 3 \downarrow, 4 \uparrow, 5 \downarrow, 6 \uparrow, 7, 8 \uparrow, 9 \downarrow\rangle + |1 \downarrow, 2 \uparrow, 3, 4 \downarrow, 5 \uparrow, 6 \downarrow, 7 \uparrow, 8, 9 \uparrow\rangle \\ &+ |1 \uparrow, 2 \downarrow, 3 \uparrow, 4, 5 \downarrow, 6 \uparrow, 7 \downarrow, 8 \uparrow, 9\rangle \end{aligned} \right]
 \end{aligned}$$

$$\begin{aligned}
|\phi_{25}\rangle &= \frac{1}{\sqrt{9}} \left[\begin{aligned} &|1\uparrow,2\downarrow,3\uparrow,4\downarrow,5,6\uparrow,7\downarrow,8,9\uparrow\rangle + |1\uparrow,2\uparrow,3\downarrow,4\uparrow,5\downarrow,6,7\uparrow,8\downarrow,9\rangle \\ &+ |1,2\uparrow,3\uparrow,4\downarrow,5\uparrow,6\downarrow,7,8\uparrow,9\downarrow\rangle + |1\downarrow,2,3\uparrow,4\uparrow,5\downarrow,6\uparrow,7\downarrow,8,9\uparrow\rangle \\ &+ |1\uparrow,2\downarrow,3,4\uparrow,5\uparrow,6\downarrow,7\uparrow,8\downarrow,9\rangle + |1,2\uparrow,3\downarrow,4,5\uparrow,6\uparrow,7\downarrow,8\uparrow,9\downarrow\rangle \\ &+ |1\downarrow,2,3\uparrow,4\downarrow,5,6\uparrow,7\uparrow,8\downarrow,9\rangle + |1\uparrow,2\downarrow,3,4\uparrow,5\downarrow,6,7\uparrow,8\uparrow,9\downarrow\rangle \\ &+ |1\downarrow,2\uparrow,3\downarrow,4,5\uparrow,6\downarrow,7,8\uparrow,9\rangle \end{aligned} \right] \\
|\phi_{26}\rangle &= \frac{1}{\sqrt{9}} \left[\begin{aligned} &|1\uparrow,2\downarrow,3\uparrow,4\downarrow,5\uparrow,6,7\downarrow,8,9\uparrow\rangle + |1\uparrow,2\uparrow,3\downarrow,4\uparrow,5\downarrow,6\uparrow,7,8\downarrow,9\rangle \\ &+ |1,2\uparrow,3\uparrow,4\downarrow,5\uparrow,6\downarrow,7\uparrow,8,9\downarrow\rangle + |1\downarrow,2,3\uparrow,4\uparrow,5\downarrow,6\uparrow,7\downarrow,8\uparrow,9\rangle \\ &+ |1,2\downarrow,3,4\uparrow,5\uparrow,6\downarrow,7\uparrow,8\downarrow,9\rangle + |1\uparrow,2,3\downarrow,4,5\uparrow,6\uparrow,7\downarrow,8\uparrow,9\downarrow\rangle \\ &+ |1\downarrow,2\uparrow,3,4\downarrow,5,6\uparrow,7\uparrow,8\downarrow,9\rangle + |1\uparrow,2\downarrow,3\uparrow,4,5\downarrow,6,7\uparrow,8\uparrow,9\downarrow\rangle \\ &+ |1\downarrow,2\uparrow,3\downarrow,4\uparrow,5,6\downarrow,7,8\uparrow,9\rangle \end{aligned} \right] \\
|\phi_{27}\rangle &= \frac{1}{\sqrt{9}} \left[\begin{aligned} &|1\uparrow,2\downarrow,3\uparrow,4\downarrow,5\uparrow,6\downarrow,7,8,9\uparrow\rangle + |1\uparrow,2\uparrow,3\downarrow,4\uparrow,5\downarrow,6\uparrow,7\downarrow,8,9\rangle \\ &+ |1,2\uparrow,3\uparrow,4\downarrow,5\uparrow,6\downarrow,7\uparrow,8\downarrow,9\rangle + |1,2,3\uparrow,4\uparrow,5\downarrow,6\uparrow,7\downarrow,8\uparrow,9\downarrow\rangle \\ &+ |1\downarrow,2,3,4\uparrow,5\uparrow,6\downarrow,7\uparrow,8\downarrow,9\rangle + |1\uparrow,2\downarrow,3,4,5\uparrow,6\uparrow,7\downarrow,8\uparrow,9\downarrow\rangle \\ &+ |1\downarrow,2\uparrow,3\downarrow,4,5,6\uparrow,7\uparrow,8\downarrow,9\rangle + |1\uparrow,2\downarrow,3\uparrow,4\downarrow,5,6,7\uparrow,8\uparrow,9\downarrow\rangle \\ &+ |1\downarrow,2\uparrow,3\downarrow,4\uparrow,5\downarrow,6,7,8\uparrow,9\rangle \end{aligned} \right]
\end{aligned}$$

The action of H' on the reduced Hilbert space, gives

$$H'|\phi_0\rangle = -t|\phi_1\rangle - t|\phi_6\rangle + \frac{J_z}{4}|\phi_0\rangle$$

$$H'|\phi_1\rangle = -t|\phi_0\rangle - t|\phi_2\rangle - t|\phi_7\rangle - t|\phi_{22}\rangle + \frac{J_z}{2}|\phi_1\rangle$$

$$H'|\phi_2\rangle = -t|\phi_1\rangle - t|\phi_3\rangle - t|\phi_8\rangle - t|\phi_{23}\rangle + \frac{J_z}{2}|\phi_2\rangle$$

$$H'|\phi_3\rangle = -t|\phi_2\rangle - t|\phi_4\rangle - t|\phi_{10}\rangle - t|\phi_{24}\rangle + \frac{J_z}{2}|\phi_3\rangle$$

$$H'|\phi_4\rangle = -t|\phi_3\rangle - t|\phi_5\rangle - t|\phi_{13}\rangle - t|\phi_{25}\rangle + \frac{J_z}{2}|\phi_4\rangle$$

$$H'|\phi_5\rangle = -t|\phi_4\rangle - t|\phi_6\rangle - t|\phi_{17}\rangle - t|\phi_{26}\rangle + \frac{J_z}{2}|\phi_5\rangle$$

$$H'|\phi_6\rangle = -t|\phi_0\rangle - t|\phi_5\rangle - t|\phi_{22}\rangle - t|\phi_{27}\rangle + \frac{J_z}{2}|\phi_6\rangle$$

$$H'|\phi_7\rangle = -t|\phi_1\rangle - t|\phi_8\rangle + \frac{3J_z}{4}|\phi_7\rangle$$

$$H'|\phi_8\rangle = -t|\phi_2\rangle - t|\phi_7\rangle - t|\phi_9\rangle - t|\phi_{10}\rangle + J_z|\phi_8\rangle$$

$$H'|\phi_9\rangle = -t|\phi_8\rangle - t|\phi_{11}\rangle + \frac{3J_z}{4}|\phi_9\rangle$$

$$H'|\phi_{10}\rangle = -t|\phi_3\rangle - t|\phi_8\rangle - t|\phi_{11}\rangle - t|\phi_{13}\rangle + J_z|\phi_{10}\rangle$$

$$H'|\phi_{11}\rangle = -t|\phi_9\rangle - t|\phi_{10}\rangle - t|\phi_{12}\rangle - t|\phi_{14}\rangle + J_z|\phi_{11}\rangle$$

$$H'|\phi_{12}\rangle = -t|\phi_{11}\rangle - t|\phi_{15}\rangle + \frac{3J_z}{4}|\phi_{12}\rangle$$

$$H'|\phi_{13}\rangle = -t|\phi_4\rangle - t|\phi_{10}\rangle - t|\phi_{14}\rangle - t|\phi_{17}\rangle + J_z|\phi_{13}\rangle$$

$$H'|\phi_{14}\rangle = -t|\phi_{11}\rangle - t|\phi_{13}\rangle - t|\phi_{15}\rangle - t|\phi_{18}\rangle + J_z|\phi_{14}\rangle$$

$$H'|\phi_{15}\rangle = -t|\phi_{12}\rangle - t|\phi_{14}\rangle - t|\phi_{16}\rangle - t|\phi_{19}\rangle + J_z|\phi_{15}\rangle$$

$$\begin{aligned}
H'|\phi_{16}\rangle &= -t|\phi_{15}\rangle - t|\phi_{20}\rangle + \frac{3J_z}{4}|\phi_{16}\rangle \\
H'|\phi_{17}\rangle &= -t|\phi_5\rangle - t|\phi_{13}\rangle - t|\phi_{18}\rangle - t|\phi_{22}\rangle + J_z|\phi_{17}\rangle \\
H'|\phi_{18}\rangle &= -t|\phi_{14}\rangle - t|\phi_{17}\rangle - t|\phi_{19}\rangle - t|\phi_{23}\rangle + J_z|\phi_{18}\rangle \\
H'|\phi_{19}\rangle &= -t|\phi_{15}\rangle - t|\phi_{18}\rangle - t|\phi_{20}\rangle - t|\phi_{24}\rangle + J_z|\phi_{19}\rangle \\
H'|\phi_{20}\rangle &= -t|\phi_{16}\rangle - t|\phi_{19}\rangle - t|\phi_{21}\rangle - t|\phi_{25}\rangle + J_z|\phi_{20}\rangle \\
H'|\phi_{21}\rangle &= -t|\phi_{20}\rangle - t|\phi_{26}\rangle + \frac{3J_z}{4}|\phi_{21}\rangle \\
H'|\phi_{22}\rangle &= -t|\phi_1\rangle - t|\phi_6\rangle - t|\phi_{17}\rangle - t|\phi_{23}\rangle + J_z|\phi_{22}\rangle \\
H'|\phi_{23}\rangle &= -t|\phi_2\rangle - t|\phi_{18}\rangle - t|\phi_{22}\rangle - t|\phi_{24}\rangle + J_z|\phi_{23}\rangle \\
H'|\phi_{24}\rangle &= -t|\phi_3\rangle - t|\phi_{19}\rangle - t|\phi_{23}\rangle - t|\phi_{25}\rangle + J_z|\phi_{24}\rangle \\
H'|\phi_{25}\rangle &= -t|\phi_4\rangle - t|\phi_{20}\rangle - t|\phi_{24}\rangle - t|\phi_{26}\rangle + J_z|\phi_{25}\rangle \\
H'|\phi_{26}\rangle &= -t|\phi_5\rangle - t|\phi_{21}\rangle - t|\phi_{25}\rangle - t|\phi_{27}\rangle + J_z|\phi_{26}\rangle \\
H'|\phi_{27}\rangle &= -t|\phi_6\rangle - t|\phi_{26}\rangle + \frac{3J_z}{4}|\phi_{27}\rangle
\end{aligned}$$

The matrix arising from nine-site chain is large (i.e 28x28 with symmetry consideration). Hence, only the results for the numerical ground state energy will be presented in section 5.

5.0 Presentation and Discussion of Results

This section presents the numerical exact result for the energy of two holes for five-, seven- and nine-site chains in the subspaces of $S_{tot}^z = 1/2$. From Table 1, it is observed that at $J_z/t = 0$ the energy of two holes for N=5 is -3.60388. This value is not in excellent agreement with that proposed by Nagaoka that the energy of a hole at $J_z=0$ must be equal to $-zt$, where z is the coordination number [23]. This is simply because the degrees of freedom for two holes in one dimension reduce from 4 to 2 whenever they are on Neighbouring sites. For this zero value of J_z , the energy of the holes is found to decrease with increase in N. *This is because at the thermodynamic limit (large N), number of degrees of freedom for the two holes approaches 2z (or 4), hence agreement with Nagaoka result of -2zt can made.* At this energy, the holes can propagate freely through the antiferromagnetic background without disrupting the spin background and expending energy. This is because the antiferromagnetic coupling J_z which provides the magnetic energy as well as the confining potential is zero. The energy of the hole is found to increase slightly in the weak coupling regime ($J_z/t \ll 1$) and sharply in the strong coupling regime ($(J_z/t \ll 1)$). This increase in the energy of the holes is due to the magnetic energy cost incurred in creating a ferromagnetic bond or a string of flipped spins. This energy cost will result to a linear rising potential that might confine the holes to their original sites. Hence, the coherent propagation of the holes might be slightly compromised as J_z is increased. In order to create a ferromagnetic bond, each of the holes must expend a magnetic energy of $J_z/2$.

For comparison with the current result for two holes, the result of the energy of a single obtained in ref. [24] is here reproduced in Table 2. At a glance, it is obvious that the energy expended by a single hole propagating in an Ising antiferromagnet is greater than that expended by two holes in the same background. This is because it is possible for two holes to minimize their energy by propagating in such a way that at every instant they are at nearest neighbour sites. In this style of propagation, the energy expended by the first hole in creating an overturned spin is easily recovered by the second hole following behind. For the single hole at $J_z/t \leq 3$, an increase in N increases the hole energy slightly. On the other hand, an increase in N causes a decrease in the energy of two holes for finite J_z . This means that at large N, two propagating holes in one dimensional antiferromagnet can minimize their energy and so maintain a smooth coherent motion.

Table 1: The energy of two holes E_h/t as a function of J_z/t for 5, 7 and 9 sites

J_z/t	E_h/t (5sites)	E_h/t (7sites)	E_h/t (9 sites)
0.00000	-3.23607	-3.60388	-3.75877
0.01000	-3.22963	-3.59604	-3.75029
0.02000	-3.22320	-3.58821	-3.74182
0.05000	-3.20394	-3.56475	-3.71644
0.10000	-3.17190	-3.52574	-3.67425
0.20000	-3.10812	-3.44813	-3.59028
0.40000	-2.98175	-3.29448	-3.42405
0.60000	-2.95695	-3.14300	-3.26020
0.80000	-2.73372	-2.99374	-3.09886
1.00000	-2.61206	-2.84676	-2.94015
1.50000	-2.31476	-2.48952	-2.55547
2.00000	-2.02715	-2.14720	-2.18882
2.50000	-1.74905	-1.81988	-1.84051
3.00000	-1.48025	-1.50734	-1.51022
4.00000	-0.96942	-0.92474	-0.90072

Table 2: The energy of one hole E_h/t as a function of J/t for 4, 6, and 8 sites

J_z/t	E_h/t (4sites)	E_h/t (6 sites)	E_h/t (8 sites)
0.00000	-2.00000	-2.00000	-2.00000
0.01000	-1.99167	-1.99100	-1.99072
0.02000	-1.98334	-1.98201	-1.98144
0.05000	-1.95838	-1.95505	-1.95362
0.10000	-1.91685	-1.91020	-1.90735
0.20000	-1.83408	-1.82082	-1.81514
0.40000	-1.66969	-1.64338	-1.63213
0.60000	-1.50688	-1.46782	-1.45121
0.80000	-1.34568	-1.29428	-1.27264
1.00000	-1.18614	-1.12291	-1.09665
1.50000	-0.79473	-0.70479	-0.66958
2.00000	-0.41421	-0.30278	-0.26308
2.50000	-0.04473	0.08215	0.12192
3.00000	0.31386	0.45002	0.48662
4.00000	1.00000	1.13919	1.16576

6.0 Conclusion

The motion of two holes in one dimensional antiferromagnetic Mott insulator within the t - J_z has been studied. The energy of two holes is found to increase with J_z . This is because magnetic energy costing $J_z/2$ is paid each time a ferromagnetic bond is created. This might have the effect of compromising the coherent motion of the holes since the string potential that tends to confine the hole is also dependent on J_z .

From Table 1 and Table 2, it is obvious that the energy expended by a single hole propagating in an Ising antiferromagnet is greater than that expended by two holes in the same background. This is because two holes can minimize their energy if their propagations keep them at nearest neighbour. In this style of propagation, the energy expended by the first hole in creating an overturned spin and hence a ferromagnetic bond is easily recovered by the second hole following the first. In this way, the original spin configuration is restored and the two holes can be conceived to be in state in state of degenerate vacuum.

From this result of the exact calculation of two holes dynamics in 1D, it obvious that hole pairing is possible for one and quasi-one dimensional Mott insulators such as Sr_2CuO_3 and SrCuO_2 . In two dimensions (2D), the motion of a single hole can create strings of flipped spins along the path of the hole, making it impossible for a hole to have a coherent propagation [25]. In the light of the results obtain here for two holes in 1D, one can naively say that hole pairing which helps to unwind strings of flipped strings is possible in 2D. High temperature Superconductivity is a low energy in which the charge carriers (hole or electrons) in the superconducting materials formed a pair and propagates in such way as to minimize their energy. Since coherent propagation is due to hole pairing, one can therefore conclude that t - J model and its variants do support superconductivity.

7.0 References

- [1] Bednorz J. G. and Müller K. A. (1986). Possible high T_c superconductivity in the Ba–La–Cu–O system. *Z. Physik*, B 64, 189–193.
- [2] Leggett A. (2006). "What DO we know about high T_c ?" *Nature Physics* 2, 134-136.
- [3] Dagotto E. (1994). Correlated electrons in high-temperature superconductors. *Rev. Mod. Phys.*, 66, 763-840.
- [4] Mott. N.F. (1949). The Basis of electron theory of metals, with special reference to the transition metals. *Proc. Phys. Soc.*62, 7-A, 416-422.
- [5] Fujisawa H., T. Yokoya and Takahashi T. (1999). Angle-resolved photoemission study of Sr_2CuO_3 . *Phys. Rev. B* 59, 7358-7362.
- [6] Kim C. (2001). Spin–charge separation in 1D Mott-insulator and related systems. *JESRP*, Vol.117-118, 503-515.
- [7] Kidd T. E., Valla T., Johnson P. D., Kim K. W., Gu G. D. and Homes C. C. (2008). Doping of a one-dimensional Mott insulator: Photoemission and optical studies of $\text{Sr}_2\text{CuO}_{3+\delta}$. *Phys. Rev. B* 77, 054503-1–7.
- [8] Guan X. W., Batchelor M. T, and Lee C. (2013). Fermi gases in one dimension: From Bethe ansatz to experiments. *Rev. Mod. Phys.* 85, 1633-1696.
- [9] Kivelson S. A., Bindloss I. P., Fradkin E., Oanesyan V., Tranquada J. M., Kapitul-nik A., and Howald C. (2003). How to detect stripes in high temperature superconductor. *Rev. Mod. Phys.*, 75, 1201-1241.

- [10] Samal D and Koster G. (2015). Manipulating oxygen sublattice in ultra thin cuprates: A new direction to engineer oxides. *Journal of Materials Research*, Vol. 30, 463-476.
- [11] Kuiper B., Samal D., Blank D.H.A., Elshof J.E. ten, Rijnders A.J.H.M. and Koster G. (2013). *Control of oxygen sublattice structure in ultra-thin SrCuO₂ films studied by X-ray photoelectron diffraction*. *APL Mat.* 1, 042113-1—6.
- [12] Karmakar K , A. Singh A. , Singh S. , Poole A , and Rüegg C. (2014). Crystal Growth of the Nonmagnetic Zn²⁺ and Magnetic Co²⁺ Doped Quasi-One-Dimensional Spin Chain Compound SrCuO₂ Using the Traveling Solvent Floating Zone Method. *Cryst. Growth Des.*, 14 (3), 1184–1192.
- [13] Zhu Z., Jiang H. C., Qi Y., Tian C. and Weng Z. Y.(2013). Strong correlation induced charge localization in antiferromagnets. *Sci. Rep.* 3, 2586-1—11.
- [14] Zhu Z., Jiang H. C., Sheng D.N. and Weng Z. Y. (2014). Nature of strong hole pairing in doped Mott antiferromagnets *Sci. Rep.* 4, 5419-1—11.
- [15] Shraiman B. I. and Siggia. E. D. (1988). Two-Particle Excitations in Antiferromagnetic Insulators. *Phys. Rev.*, B60, 740-743.
- [16] Prelovšek P., Sega I. and Bonča. (1990) Cummulant-expansion study of holes in quantum antiferromagnet. *Phys. Rev.* B42, 10706-10713.
- [17] Singh R. J, Khan S. (2014). Hole-Pair Formation in Cuprate Superconductors despite Antiferromagnetic Fluctuations. *World Journal of Condensed Matter Physics*, 4, 141-152.
- [18] Trugman S.A. (1988). Interaction of holes in a Hubbard antiferromagnet and high-temperature superconductivity. *Phys. Phys. Rev.* B37, 1597-1603.
- [19] Lin H. Q., Hirsch J. E., and Scalapino D. J. (1988). Pairing in the two-dimensional Hubbard model: An exact diagonalization study. *Phys. Rev. B* 37, 7359 -7367.
- [20] Ronning F., Shen K. M., Armitage N. P., Damascelli A., Lu D.H., Shen Z.-X., Miller L. L. and Kim C.(2005). Anomalous high-energy dispersion in angle-resolved photoemission spectra from the insulating cuprate Ca₂CuO₂Cl₂ . *Phys. Rev.B* 71, 094518-1—5.
- [21] Graf J., Gweon G.-H., McElroy K., Zhou S. Y., Jozwiak C., Rotenberg E., Bill A., Sasagawa T., Eisaki H., Uchida S., Takagi H., Lee D.-H., and Lanzara A. (2007). A universal high energy anomaly in angle resolved photoemission spectra of high temperature superconductors – possible evidence of spinon andholon branches. *Phys. Rev. Lett.*98, 067004-1--4
- [22] Manuosakis E. (2007). String excitations of a hole in a quantum antiferromagnet and photoelectron Spectroscopy. *Phys. Lett. A* 362, 86-89.
- [23] Nagaoka Y. (1966). Ferromagnetism in a Narrow, Almost Half-Filled S Band. *Phys. Rev.* B147, 392 – 405.

- [24] Ehika S. and Idiodi J.O.A. (2012). The dynamics of a hole in two dimensional Mott insulators. Journal of NAMP Vol. 21, 1-10.

- [25] Ehika S. and Idiodi J.O.A. (unpublished). Possibility of hole confinement in the weak coupling regime of finite one dimensional Ising antiferromagnet and the emergence of spin-charge separation in the bulk limit